CrystEngComm

Accepted Manuscript

ROYAL SOCIETY OF CHEMISTRY

www.rsc.org/crystengcomm

Journal Name

ARTICLE

Isoskeletal Schiff Base Polynuclear Coordination Clusters: Synthetic and Theoretical Aspects

Received 00th January 20xx,
Accepted 00th January 20xx

DOI: 10.1039/x0xx00000x

X`www.rsc.org/

Kieran Griffiths, Vassiliki N. Dokorou, John Spencer, Alaa Abdul-Sada, Alfredo Vargas* and George E. Kostakis*

This work addresses and enlightens synthetic aspects derived from our effort to systematic construct isoskeletal tetranuclear Coordination Clusters (CCs) of a general formula $[TR_2Ln_2(\mathbf{LX})_4(NO_3)_2(solv)_2]$ possessing the specific defected dicubane topology, utilizing various substituted Schiff Base organic ligands ($H_2\mathbf{LX}$) and $Ni^{II/}Co^{II}$ and $Dy(OTf)_3$ salts. Our synthetic work is further supported by DFT studies.

Introduction

The chemistry of polynuclear Coordination Clusters (CCs)[1,2] of paramagnetic 3d and/or 4f metals is an area of research that offers many interdisciplinary opportunities to connect with chemistry, physics, biology and materials science. Aesthetically pleasing structures have been reported,[3–12] moreover several research groups are showcasing the relevance of CCs in a variety of fields such as catalysis,[13–16] biology,[17] luminescence,[18–20] magnetic resonance[21] and molecular magnetism.[22,23]

Several organic ligands have been employed to build new CCs[24] and among them Schiff base ligands are widely employed to give access to a plethora of compounds with unprecedented topologies and interesting magnetic properties.[5,8,9,25–45] The reason for the widespread selection of Schiff bases as ligands for the construction of polynuclear CCs is manifold; a) their facile synthesis and readily tuneable structures obtainable in high yields, b) structural diversity is assured given the availability of a plethora of carbonyl and amine precursors and c) the accessibility of several coordination sites allows for varied binding modes, although, the exact structure and composition of the final product is invariably unpredictable. (*E*)-2-(2-Hydroxy-3-methoxybenzylideneamino)phenol $\mathbf{H_2L1}$ (Scheme 1, left) derives from the condensation of o-vanillin and 2-aminophenol and several CCs bearing this ligand have been reported.[46–57] The blending of this ligand with Co^{II} or Ni^{II} and 4f nitrate salts, results in tetranuclear CCs[46,47] of a general formula $[TR_2Ln_2\mathbf{L1}_4(NO_3)_2(solv)_2]$, where TR is Co^{II} or Ni^{II}, Ln is Dy^{III} or Tb^{III} and solvent is THF or DMF, possessing a defected dicubane or "butterfly"[58] core (Scheme 1, middle) or **2,3M4-1** (Scheme 1, right) [48,59,60] topology with the 4f ions in the wings and the 3d metal in the hinge. This topology represents one of the most familiar structural motifs in magneto chemistry, and CCs of this type have been well-studied and their behaviour is often very well-understood.[46,47] From a structural point of view, it is worth emphasizing that $\mathbf{H_2L1}$ supports this topology in the absence of any additional bridging atom.

For a long time, synthetic chemists employed new organic ligands along with 3d and/or 4f centres, under various reaction conditions, to afford new polynuclear species, however few researchers have focused their efforts on tuning the periphery of the organic ligands and studying its influence on the properties of the final product. For example, Murugesu et al[35] reported a 7-fold enhancement on the energy barrier, U_{eff}, of a Dy^{III}_2 that behaves as Single Molecule Magnet (SMM), by introducing electron-withdrawing terminal ligands.

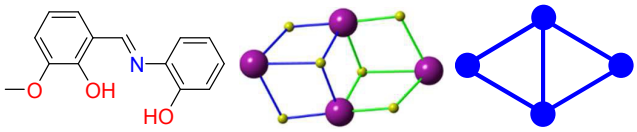

Scheme 1 (left) The (E)-2-(2-hydroxy-3-methoxybenzylideneamino)phenol $\mathbf{H_2L1}$ ligand (middle) defected dicubane motif, (right) the **2,3M4-1** topology

Having all this in mind, we initiated a project towards the synthesis of tetranuclear CCs of a general formula $[TR_2Ln_2\mathbf{L1}_4(NO_3)_2(solv)_2]$, that possess the **2,3M4-1** topology, using Co^{II} or Ni^{II} and 4f ions and substituted Schiff base ligands, similar to $\mathbf{H_2L1}$ (Scheme 2, left) in the presence or not of substituted monocarboxylates as co-ligands (Scheme 2, right). The interest for this specific motif, that is supported only from the organic ligand in the absence of any additional bridging atom, is manifold: a) These type of molecules exhibit SMM behaviour [46,47] and thus it is anticipated that the introduction of electron withdrawing groups would improve their magnetic properties. b) Replacement of the 3d and 4f ions with luminescent elements such as Zn^{II} and Eu^{III} or Tb^{III}, respectively, may lead to a new generation of materials with interesting optical properties. c) We recently showed that three tetranuclear CCs formulated as $[TR^{II}_2Dy^{III}_2(\mathbf{L1})_4(EtOH)_6](ClO_4)_2$ 2(EtOH) where TR is Co^{II} (**1**) or Ni^{II} (**2**) and $[Ni^{II}_2Dy^{III}_2(\mathbf{L1})_4Cl_2(CH_3CN)_2]\cdot 2(CH_3CN)$ (**3**) display efficient homogeneous catalytic behaviour in the room-temperature synthesis of trans-4,5-diaminocyclopent-2-enones from 2-furaldehyde and primary or secondary amines under a non-inert atmosphere and, thus, further tuning of the organic periphery may improve their catalytic performance.[57] d) More importantly, the possibility of exchanging the 3d and/or the 4f element with diamagnetic metal centres and retaining at the same time the structural topology into the solution, gives the opportunity to study

[a] Department of Chemistry, School of Life Sciences, University of Sussex, Brighton BN1 9QJ, UK. e-mail: Alfredo.Vargas@sussex.ac.uk, G.Kostakis@sussex.ac.uk

† Footnotes relating to the title and/or authors should appear here.

Electronic Supplementary Information (ESI) available: [Crystallographic Table of all compounds, ESI-MS of Compounds **7**, **10** and **16**, Protocols for Thermal and Microwave-Mediated Synthesis of Ligands, ^1H and ^{13}C NMR of Ligands FT-IR of

these molecules in the solid and/or solution state with several spectroscopic techniques such as NMR (^{1}H, ^{13}C, ^{89}Y) or EPR for the Gd species.

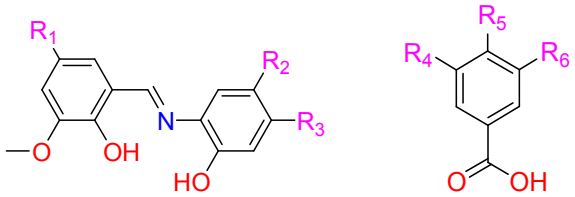

Scheme 2 (left) The substituted organic ligands used in this work R_1 = H, Br, allyl, NO_2, R_2 = H, Cl, C_6H_5, R_3 = H, NO_2, R_2-R_3 = C_4H_4, (right) the substituted monocarboxylates used in this work (**M1** R_4=R_6=NO_2, R_5 =H, **M2** R_4=NO_2 R_5=R_6=H).

Adopting the isoreticular concept, introduced by O'Keeffe and Yaghi in Metal Organic Framework chemistry,[61] a terminology that is not valid for finite structures, and since the isostructural and isomorphous terms do not fully describe the targeted CCs, we introduce herein the term "isoskeletal", previously used to describe clusters that possess the same topology[62,63] or related organic structures with the same host framework but different guests,[64,65] to describe the targeted CCs constructed from organic ligands that provide a similar coordination environment and underlying the same **2,3M4-1** topology. This work addresses and enlightens synthetic and theoretical aspects derived from our effort to systematically construct isoskeletal CCs of a general formula $[TR_2Ln_2(\mathbf{LX})_4(NO_3)_2(solv)_2]$, possessing the desired **2,3M4-1** topology. Magnetic, luminescent and catalytic studies of a few of the reported compounds will be discussed in future articles. To the best of our knowledge such a systematic synthetic and theoretical investigation for the given Ni^{II}-Co^{II}/Dy^{III} species bearing the **2,3M4-** topology has never been carried out.

Results and discussion

The synthesis of the substituted organic molecules represents the initial synthetic part of this project. A typical synthesis of a Schiff base ligand takes place in an alcoholic solution in the presence or not of a catalyst (acid or base), although other synthetic methods such as microwave-mediated [66] or solvent-free mechanochemical synthesis[67,68] can be employed. Our attempts to synthesize the substituted organic molecules bearing electron withdrawing groups (Scheme 2, left) (Table 1, entries 2 - 20) via a typical synthesis, *viz*. reflux in alcoholic solution of equivalent amounts of the corresponding aldehyde and amine, resulted in the desired products, but in very low yields. Microwave-assisted organic synthesis (MAOS) enables the rapid synthesis of organic molecules, often with excellent yields and selectivity. Interestingly, by applying MAOS[69,70] for the synthesis of the corresponding organic molecules, the yield increases drastically. In total we synthesized 19 new organic ligands (Table 1, entries 2 - 20) and we characterized via single crystal X-ray crystallography two examples, **H_2L3** and **H_2L19** (Figure 1). Single crystal X-ray studies at 173K reveal that both **H_2L3** and **H_2L19** are a mixture of keto-enol tautomers. In **H_2L3** (Figure 1 above), where two molecules can be found in the asymmetric unit, the enol form of the ligand is indicative of the existence of protons H3 and H8A that could be freely refined with chemical occupancy 22 and 23%, respectively. However, to obtain a suitable structure solution, both protons were restrained to have 25% occupancy and their O – H bond distance to be at 0.88Å. The C – O bond distances are 1.282(3) and 1.282(3) Å which are slightly higher than a typical C = O double bond. Similarly, for ligand **H_2L19**, protons H1 and H2 (Figure 1 below) could be freely refined and have 79% and 21% occupancies, indicating a 79/21 existence of ketonic / enolic form, while the C – O bond distance is 1.285(2) Å. These findings are in line with recently previously reported compounds.[67] Solution studies (^{1}H and ^{13}C NMR) of the synthesized compounds, revealed the existence of both keto and enol forms.

Table 1 A list of all substituted Schiff bases synthesized for this study. R_1, R_2 and R_3 correspond to the substituted groups seen in Scheme 2 left.

Entry		R_1	R_2	R_3	Yield (%)
1	**H_2L1**	H	H	H	95
2	**H_2L2**	H	H	NO_2	66 [96][a]
3	**H_2L3**	H	Cl	NO_2	76 [95][a]
4	**H_2L4**	H	C_6H_5	H	91
5	**H_2L5**	H	C_4H_4		88
6	**H_2L6**	NO_2	H	H	93
7	**H_2L7**	NO_2	H	NO_2	94
8	**H_2L8**	NO_2	Cl	NO_2	80
9	**H_2L9**	NO_2	C_6H_5	H	92
10	**H_2L10**	NO_2	C_4H_4		74
11	**H_2L11**	allyl	H	H	70 [98][a]
12	**H_2L12**	allyl	H	NO_2	72
13	**H_2L13**	allyl	Cl	NO_2	70
14	**H_2L14**	allyl	C_6H_5	H	69
15	**H_2L15**	allyl	C_4H_4		61 [95][a]
16	**H_2L16**	Br	H	H	84
17	**H_2L17**	Br	H	NO_2	79
18	**H_2 L18**	Br	Cl	NO_2	35 [85][a]
19	**H_2L19**	Br	C_6H_5	H	83
20	**H_2L20**	Br	C_4H_4		79

[a] MW technique

The synthesis of the targeted tetranuclear CCs represented the next part of this project. Based on the synthetic protocols that resulted in the isolation of the targeted tetranuclear CCs $[TR_2Ln_2(\mathbf{LX})_4(NO_3)_2(solv)_2]$,[57] and bearing in mind that a subtle change in the synthetic procedure may affect the shape, dimensionality and nuclearity of the final product, we screened several molecular ratios to isolate the corresponding-targeted isoskeletal CCs. At this point, it is worth mentioning that in order to avoid complicating the synthetic procedures we employed only $Dy(OTf)_3$ as the lanthanide source. During this screening procedure several interesting and unexpected results were obtained, grouped and presented below.

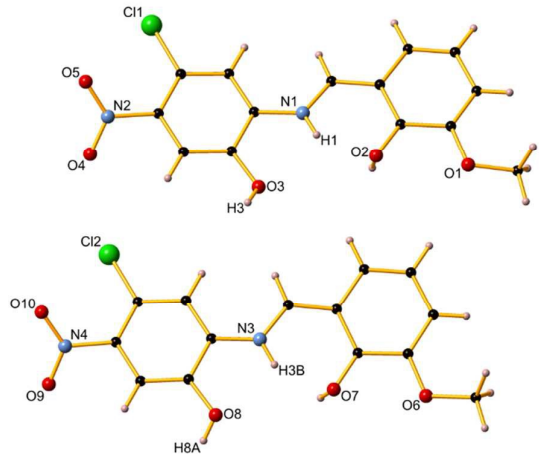

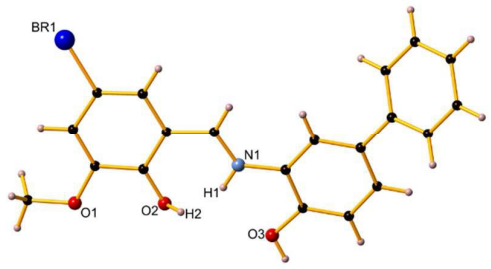

Figure 1. A schematic representation of H_2**L3** (up) and H_2**L19** (bottom) ligands.

A) Oxidation. Reaction of H_2**L6** with $Co(ClO_4)_2$, and $Dy(OTf)_3$ and Et_3N in the molar ratio 2:1:1:5 in MeOH resulted, after 3 days, in approximately 82% yield, in dark-red shaped crystals formulated as $(Et_3NH)[Co^{III}(\mathbf{L6})_2]\cdot 3MeOH$ [**4**·3MeOH] (Figure 2 left). Similarly, reaction of H_2**L20** with $Co(ClO_4).6H_2O$ and $Dy(OTf)_3$ and Et_3N in the molar ratio 1:1:1:3 in MeOH resulted, after 6 days, in approximately 82% yield dark in red shaped crystals formulated as $(Et_3NH)[Co^{III}(\mathbf{L20})_2]\cdot 2MeOH$ [**5**·2MeOH]. (Figure 2, right). In the cases of **4** and **5**, during crystallization, upon standing at room temperature, Co^{II} is oxidized to Co^{III}. To target for the isoskeletal **2,3M4-1** Co^{II} analogues, it is important to perform the synthesis and crystallization under inert atmosphere conditions.

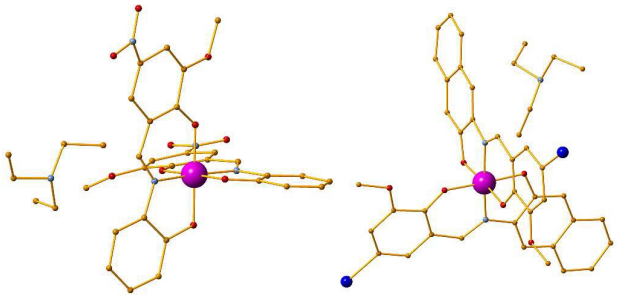

Figure 2. (left) The crystal structure of compound **4**. (right) The crystal structure of compound **5**. Solvent molecules and H-atoms are omitted for clarity Colour Code Co (pink), N (light blue), O (red), C (orange), Br (blue)

B) Solvent influence. As anticipated, modification of the organic periphery of the parent organic ligand H_2**L1** drastically affects its solubility. However, when targeting for the corresponding isoskeletal tetranuclear species, the use of a mixture of solvents, to enhance dissolving, results in the formation of undesired compounds. For example, the reaction of ligand H_2**L14** with $Ni(ClO_4)_2$, $Dy(OTf)_3$ and Et_3N in the molar ratio 2:1:1:5 in a mixture of $EtOH/CH_2Cl_2$ results in the synthesis of a tetranuclear compound formulated as $[Ni^{II}_2Dy^{III}_2(\mathbf{L14})_4(allyl\text{-}o\text{-}vanillin)_2(EtOH)_2]\cdot 3CH_2Cl_2$ [**6**·$3CH_2Cl_2$] (Figure 3, **A**). The two allyl-o-vanillin moieties derive from the disassembling of H_2**L14** during the reaction. Interestingly, performing a similar reaction, in solely, DMF results in the formation of the desired $[Ni^{II}_2Dy^{III}_2(\mathbf{L14})_4(DMF)_6]$ $2(ClO_4)$ 4DMF [**7** 4DMF] (Figure 3). This observation was additionally proven by performing a reaction of ligand H_2**L19** with $Ni(ClO_4)_2.6H_2O$ and $Dy(OTf)_3$ and Et_3N in the molar ratio 2:1:1:5 in a mixture of $EtOH/CH_2Cl_2$, which resulted in the isolation of compound $[Ni^{II}_2Dy^{III}_2(\mathbf{L19})_4(bromo\text{-}o\text{-}vanillin)_2(EtOH)_2]$ 6EtOH [**8**·6EtOH] (Figure 3). Moreover, utilizing a blend of EtOH/THF in the following reaction $Ni(ClO_4)_2.6H_2O$, $Dy(OTf)_3$ and Et_3N in the molar ratio 2:1:1:5 results in $[Ni^{II}_2Dy^{III}_2(\mathbf{L15})_4(allyl\text{-}o\text{-}vanillin)_2(EtOH)_2]$ 2THF 2EtOH [**9** 2THF 2EtOH] (Figure 3). However, performing a similar reaction in DMF results in the formation of the desired compound $[Ni^{II}_2Dy^{III}_2(\mathbf{L15})_4(DMF)_2]$ $2(ClO_4)$ [**10**] (Figure 3). The aforementioned examples indicate that the use of a second solvent increases the chances of the formation of a by-product and thus the mixture of solvents may not correspond to an ideal synthetic protocol when targeting high purity compounds.

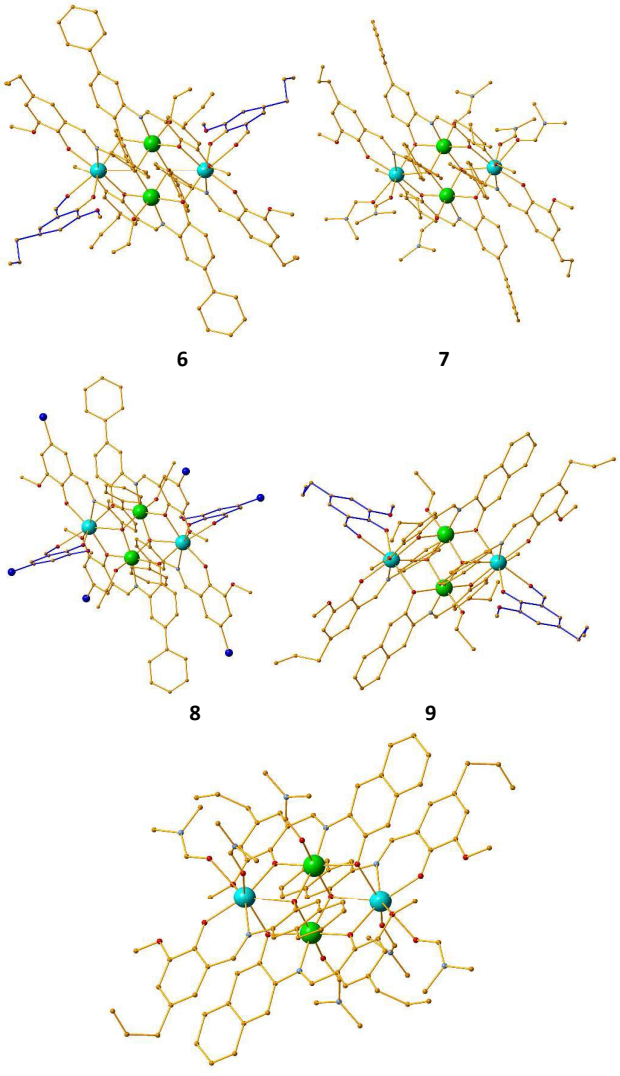

Figure 3. The crystal structures of compounds **6** – **10**. H atoms and solvents are omitted for clarity. The substituted o-vanillin moiety is indicated with blue colour. Colour Code Ni (light green), Dy (light blue), N (blue), O (red), C (orange), Br (blue)

C) Solvent concentration influence. During our efforts to scale up the synthesis of compound **2**,[57] we performed reactions with a lower amount of solvent (10ml instead of 20ml) or we tripled the amount of the reactants retaining the same the molar ratio, but then a different product was obtained, formulated as $[Ni^{II}_2Dy^{III}_2(\mathbf{L1})_4(EtOH)_4(H_2O)_2](ClO_4)_2$ (**11**) (Figure 4). Two water molecules coordinate to Ni^{II} centres in **11**, in contrast to two ethanol molecules found in **2**.[57] Moreover, performing a similar scale up reaction in a different solvent such as DMF another compound is formed formulated as $[Ni^{II}_2Dy^{III}_2(\mathbf{L1})_4(DMF)_6](OTf_3)_2\cdot 2DMF$ (**12**·2DMF) (Figure 4), instead of

the expected perchlorate derivative. In addition, performing a concentrated reaction of $Ni(ClO_4)\cdot 6H_2O$, $Dy(OTf)_3$, Et_3N and **H_2L20** in the molar ratio 1:1:2:8 resulted in a CC with the formula $[Ni^{II}_2Dy^{III}_2(\mathbf{L20})_4(DMF)_6]$ $[Ni^{II}_2Dy^{III}_2(\mathbf{L20})_4(DMF)_4(H_2O)_2]$ $4(ClO_4)$ 5DMF (**13**·5DMF). (Figure 4)

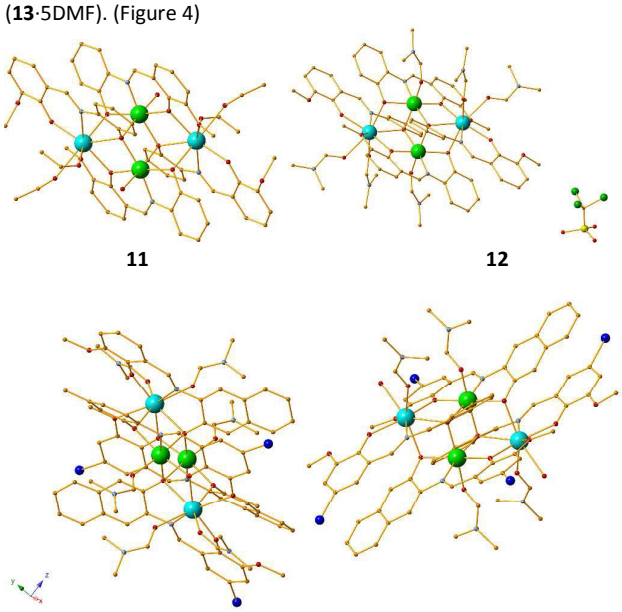

Figure 4. The crystal structures of **11** (A), **12** (B) and **13** (C). Colour Code Ni (light green), Dy (light blue), N (blue), O (red), C (orange), Br (blue), F (green) S (yellow)

D) Molar Ratio. Reaction of $Ni(ClO_4)_2$ $6(H_2O)$, $Dy(OTf)_3$, **H_2L5** with Et_3N in MeOH in the molar ratio 1:1:2:5 resulted in the isolation of a tetranuclear cubane Ni_4 formulated as $[Ni^{II}_4(\mathbf{L5})_4(MeOH)_4]$ ·6MeOH (**14** · 6MeOH) which is isoskeletal to the tetranuclear cubic Ni_4 CC formed by **H_2L1** ligand, reported recently.[54] However, performing the same reaction in EtOH, results in the isolation of the targeted isoskeletal tetranuclear $[Ni^{II}_2Dy^{III}_2(\mathbf{L5})_4(EtOH)_6]$ $2(ClO_4)$ · 4EtOH (**15** · 4EtOH) (Figure 5).

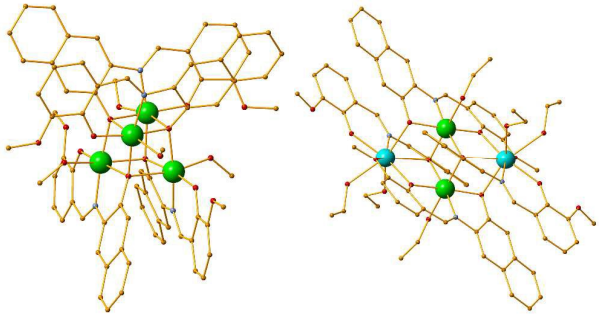

Figure 5. The crystal structures of compounds **14** (left) and **15** (right). Colour Code Ni (light green), Dy (light blue), N (blue), O (red), C (orange)

E) Solvent diffusion crystallization. In our effort to obtain the targeted tetranuclear $Ni^{II}_2Dy^{III}_2$ analogues with **H_2L4** as a ligand via the diffusion crystallization technique, a compound formulated as $[Ni^{II}_2Dy^{III}_2(\mathbf{L4})_4(DMF)_6]$ $2(ClO_4)$ ·$2Et_2O$ (**16** ·$2Et_2O$) (Figure 6, left) which contains two ether molecules as lattice solvent, was isolated.[71–74] Upon standing at room temperature, compound **16**, immediately loses its crystallinity.

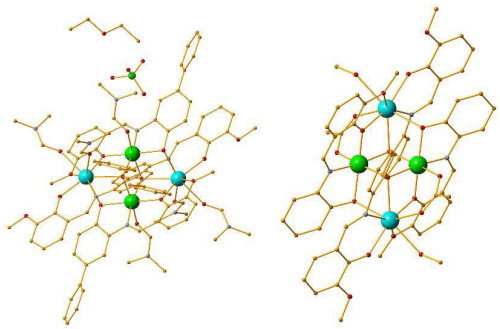

Figure 6. The crystal structure of compound **16** (left) and **17** (right). Colour Code Ni (light green), Dy (light blue), N (blue), O (red), Cl (light green),

F) Co-ligand introduction. To identify the possibility of introducing a monocarboxylate group as a co-ligand on the periphery of the **2,3M4-1** motif, we performed a pilot reaction with **H_2L1**, $Ni(OAc)_2$ $4(H_2O)$, $Dy(OTf)_3$ and Et_3N in the molar ratio 2:1:1:2 in MeOH that resulted in the isolation of a compound formulated as $[Ni^{II}_2Dy^{III}_2(\mathbf{L1})_4(OAc)_2(MeOH)_2]$ ·2MeOH (**17** · 2MeOH) (Figure 6, right). Each acetate group bridges the Ni and Dy centres, which is in contrast with the NO_3 analogues that prefer to chelate to the Ln centres.[46,47]

Employment of the bulky co-ligands **M1** and **M2** along with ligand **H_2L12** and $Co(ClO_4)_2 \cdot 6H_2O$ and $Dy(OTf)_3$ in the molar ratio of 2:1:1:5 in N,N'-DMF as solvent results in the isolation of two compounds formulated as $[Co^{II}_2Dy^{III}_2(\mathbf{L12})_4(\mathbf{M1})_2(DMF)_2]$ (**18**) and $[Co^{II}_2Dy^{III}_2(\mathbf{L12})_4(\mathbf{M2})_2(DMF)_2]$ · 2DMF (**19**·2DMF), respectively (Figure 7).

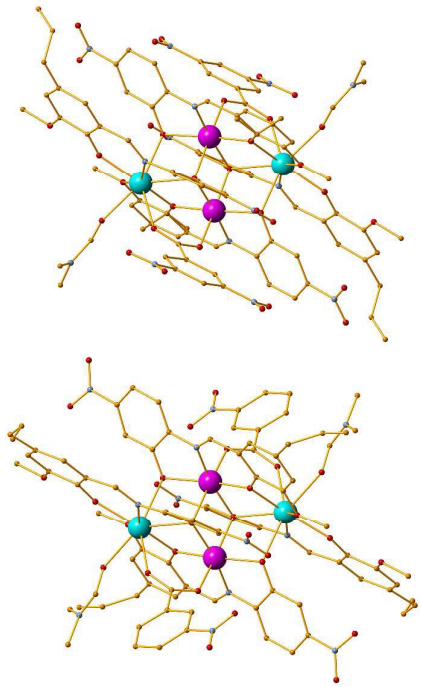

Figure 7. The crystal structure of compounds **18** (upper) and **19** (lower). Colour Code Co (pink), Dy (light blue), N (blue), O (red), C (orange)

However, our effort to obtain the isoskeletal to **18** $Co^{II}_2Dy^{III}_2$ compound along with ligand **H_2L2** instead of **H_2L12** by performing a similar reaction resulted in red plate crystals formulated as $[Dy^{III}(\mathbf{M1})_3(DMF)_2]$ (**20**) (Figure 8). Compound **20** is a one

dimensional (1D) coordination polymer and can be considered as polymorph to the recently reported compound.[75]

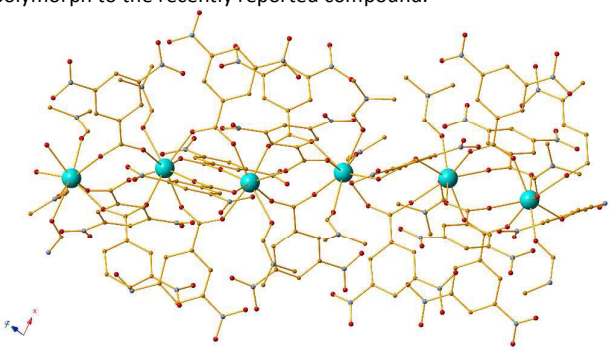

Figure 8. The crystal structure of compound **20.** Colour Code Dy (light blue), N (blue), O (red), C (orange)

Finally, the diffusion of Et_2O to a concentrated reaction of ligand **H_2L5** along with $Ni(ClO_4)\cdot 6H_2O$, $Dy(OTf)_3$, **M1** and Et_3N in DMF results in the formation of a compound formulated as $[Ni^{II}_2Dy^{III}_2(OH)(\mathbf{L5})_3(\mathbf{M1})_3(DMF)_2] \cdot 1.5DMF \cdot Et_2O$ (**21**·1.5DMF·Et_2O) which possess the **2,3M4-1** topology. Surprisingly, only three organic ligands are involved in the aggregation in contrast to four ligands used in compounds **6** - **19**. The skeleton of **21** is further supported by the presence of a hydroxyl μ_3-OH group. Also, one Et_2O molecule is trapped in the lattice.

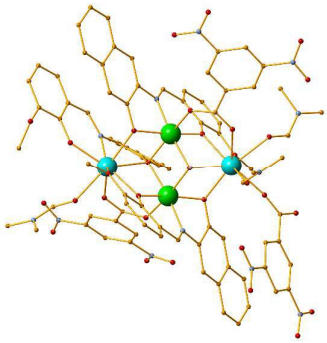

Figure 9. The crystal structure of compound **21**. Colour Code Ni (light green), Dy (light blue), N (blue), O (red), C (orange), H (white)

Solution studies. To further confirm the identity of compounds **7**, **10** and **16** in solution, we performed electrospray ionization mass (ESI-MS) spectrometry study. For **7**, we observed three peaks in the MS (positive-ion mode) at m/z 1009.2113, 972.1730 and 936.1485 which correspond perfectly to three dicationic fragments, $[Ni^{II}_2Dy^{III}_2(\mathbf{L14})_4(DMF)_2]^{2+}$. $[Ni^{II}_2Dy^{III}_2(\mathbf{L14})_4(DMF)]^{2+}$ and $[Ni^{II}_2Dy^{III}_2(\mathbf{L14})_4]^{2+}$, respectively. (see Figures S1 ESI). Similarly, for **10**, peaks at m/z 1742.2549, 876.6074, 840.0702 and 803.067 correspond to $[Ni^{II}_2Dy^{III}_2(\mathbf{L15})_4(MeOH)]^{+}$, $[Ni^{II}_2Dy^{III}_2(\mathbf{L15})_4(DMF)_2]^{2+}$, $[Ni^{II}_2Dy^{III}_2(\mathbf{L15})_4(DMF)]^{2+}$ and , $[Ni^{II}_2Dy^{III}_2(\mathbf{L15})_4]^{2+}$ fragments (see Figures S2), respectively. For compound **16**, the following four m/z 1847.228, 929.1356, 892.1121 and 855.5781 peaks correspond to $[Ni^{II}_2Dy^{III}_2(\mathbf{L4})_4(MeOH)]^{+}$, $[Ni^{II}_2Dy^{III}_2(\mathbf{L4})_4(DMF)_2]^{2+}$, $[Ni^{II}_2Dy^{III}_2(\mathbf{L4})_4(DMF)]^{2+}$ and , $[Ni^{II}_2Dy^{III}_2(\mathbf{L4})_4]^{2+}$ fragments (see Figures S3), respectively. However, all the efforts to obtain similar ESI-MS spectra for compounds **18** and **19,** which contain a co-ligand, were not successful.

Theoretical studies. To gain further insight into the tuning and modulation of, *inter alia*, the catalytic activities of the tetranuclear CCs, computational studies were carried out. Specifically, the influence of the organic ligands on the electronic properties of the metals was studied. The reason for this study is that the 'activity' of the ligands may be tuned by employing diverse functional groups at specific sites/positions. In order to do this, quantitative and qualitative metrics of the functional group effects were established and in parallel several congeners of the ligands were examined; more so, several model systems of the polynuclear coordination clusters were used. With respect to Scheme 2 (see text) concerning the numbering, the following tables (Tables 2 – 5) indicate the model systems studied. Figure 10 shows the visualization of the mapped molecular electrostatic potential in ligands L1m to L12m, as in the usual molecular electrostatic potential (MEP) rendering, with blue zones depicting 'positively' charged zones while red zones the 'negatively charged zones'.

One way to assess the effect of the electron withdrawing groups on the Schiff base is to qualitatively render the MEP mapped onto the van der Waals surface. Indeed, the nature of the R groups has a profound effect on the surface charge of the base on its 'inner cove' – that is, the O-O-N-O core pattern directly interacting with the metals. Figure 10 and Table 5 qualitatively illustrate this idea. Unsurprisingly, results show charge distribution along the cove can indeed be modulated upon modification of the groups.

Table 2. Recapitulative table of the model ligands used

L	R_1	R_2	R_3
L1m	H	H	H
L2m	OMe	H	H
L3m	$N(CH_2CH_3)_2$	H	H
L4m	F	H	H
L5m	H	H	NO_2
L6m	$CH_2CH{=}CH_2$	H	NO_2
L7m[1]	NO_2	H	H
L8m	NO_2	H	H
L9m	H	Cl	NO_2
L10m	Br	H	NO_2
L11m	NO_2	H	NO_2
L12m	NO_2	Cl	NO_2
L7: An additional NO_2 is substituted at the ortho position adjacent to R_2.			

Table 3. Recapitulative table of the co-ligands used

coL	R_4	R_5	R_6
coL1m	H	H	H
coL2m	H	F	H
coL3m	NO_2	H	NO_2

Table 4. Recapitulative table of the models used

model	M1	M2	L	coL	S
m1 11	Zn	Y	L1m	coL2m	$(CH_3)_2NCOH$
m2 11a	Ni	Y	L1m	coL2m	$(CH_3)_2NCOH$
m3 12	Zn	Y	L5m	MeOH	NO_3
m4 12a	Ni	Y	L5m	MeOH	NO_3
m5 13	Zn	Y	L1m	EtOH[1]	--
m6 14	Zn	Y	L6m	coL3m	S1m
m7 14b	Zn	Y	L1m	coL3m	S1m

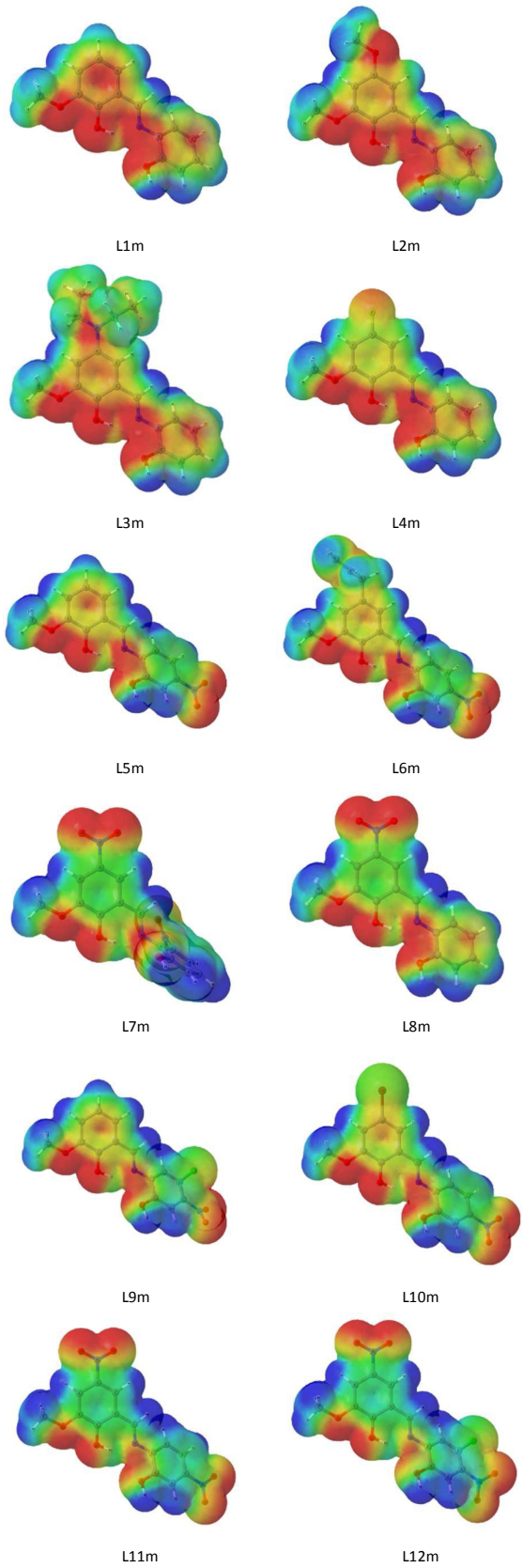

Figure 10: Rendition of the molecular electrostatic potential (MEP) of the model ligands.

In the gas phase, in their most stable geometrical configuration, the most 'simple' functionalization, i.e. having $R_1 = R_2 = R_3 = H$ turns out to confer the most of negative charge accumulation on the ligand 'anchor' points, the least being with $R_1 = NO_2$, $R_2 = Cl$, $R_3 = NO_2$. Interestingly, for a given R_1, changing R_3 has a profound effect on the charge distribution as can be illustrated by considering L1m and L5m. On the other hand, for a given R_3, changing R_1 does not have a noticeable altering effect, as shown for example by L5m versus L10m and L1m versus L2m. More crucially, the conformation of the ligand, although not surprising, ultimately determines the extent, nature and motifs of interaction between the metal-interacting side of the ligands and the metals (see figure 11). Indeed, single point (sp) calculations on L6m in its ligand-bound geometry exhibits a different charge distribution signature with respect to that of its gas-phase optimized structure (gp). The geometries differ by having the nitrogen-bound aryl group (ring 2) rotated clockwise (gp) or counter clockwise (sp) around the N-C(aryl) bond. This observation can be rationalized when one considers the frontier molecular orbitals (MO).

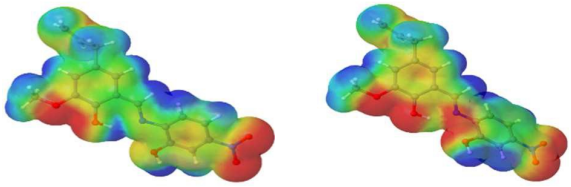

Figure 11: Rendition of the molecular electrostatic potential (MEP) of L6m in its ligand-bound (left) and in its free conformation (right).

Indeed, inspection of the LUMO – HOMO-2 of the L6m (sp) indicates that the molecular orbitals (MO) are mainly consisted of π network running throughout the whole of the molecule, even more remarkable is the low mixing of atomic p orbitals perpendicular to the molecular plane defined by ring 1 (the aryl containing R1) and the N-centered p orbital that is parallel to this plane (see Figure 12). This very orientation of the p orbital should also be responsible for the dependence of the cove charge distribution on the orientation of the hydrogens on the OH functions on both rings (data not shown).

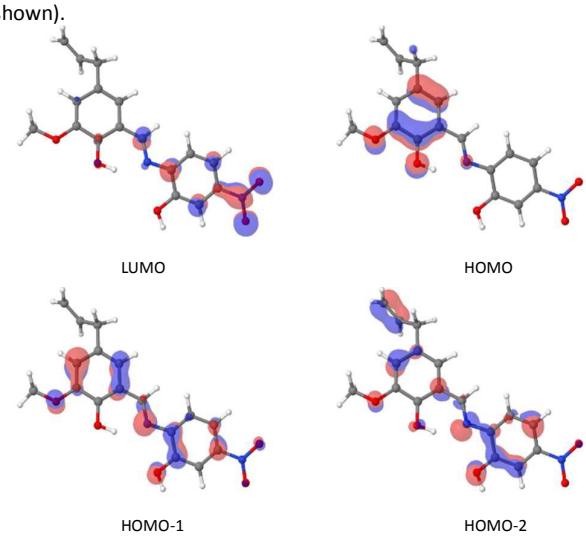

Figure 12: Frontier orbitals of L6m (sp).

In terms of partial atomic charge, within the Mulliken partitioning scheme, it can be noted that there are indeed variations in values on the metals, on the two oxygen and the nitrogen atoms (see Table 5) depending on the makeup of the ligand. Close examination suggests that, in terms of partial charges, both M2 (Table 4) and O1 (phenolic oxygen atom of o-vanillin moiety) are spectator elements and the value of their partial charge does not depend on that of the other atoms. However, an interdependence of the values of partial charge on N, O2 (phenolic oxygen atom of aminophenol moiety) and M1, can be found. The largest of such variations occurs for metal M1 and is observed between model m2 11a and model m3 12. These results are perfectly in line with that of the charge distribution being dependent on the orientation of ring 2.

Table 5. Mulliken charges

model	q(M1)	q(M2)	q(O1)	q(N)	q(O2)
m1 11	0.79	1.49	-0.64	-0.20	-0.61
m2 11a	0.53	1.49	-0.61	-0.16	-0.59
m3 12	0.93	1.34	-0.55	-0.26	-0.73
m4 12a	0.69	1.36	-0.62	-0.17	-0.58
m5 13	0.86	1.32	-0.56	-0.30	-0.73
m6 14	0.85	1.56	-0.55	-0.27	-0.70
m7 14b	0.85	1.55	-0.56	-0.27	-0.71

The above results clearly show the richness of the chemistry of the present coordination clusters: the nature of metal M1 and the identity of the R groups in the ligands play preponderant roles in both the tuning and control of the behaviour of the clusters. With the trends and rationales hereby demonstrated, it should be possible in future work to better modulate the activity of the clusters through tuning of electronic structure and control of structural constraints.

Conclusions

In this work we present the synthesis of nineteen new substituted Schiff base organic ligands and eighteen new CCs. Adopting the MOF isoreticular concept, we introduce herein the term "isoskeletal" which ideally describes structural and topological similarities found in compounds **6** – **13**, **15** – **19** and **21**. Microwave synthesis has proven to be very efficient for the synthesis of the substituted Schiff Base ligands.[76] Targeting to synthesize such isoskeletal species, it is shown that several parameters must be taken into account. We do show here that slight change in the synthetic procedure affect drastically the formula of the desired compound. However, the usage of different lanthanide sources and the lanthanide contraction are two parameters that have not been taken into account in this study and are anticipated to have a major impact in the shape, nuclearity and formula final product. The possibility of producing isoskeletal species and exchanging the 3d and/or the 4f element with diamagnetic elements such as Zn^{II} or Y^{III}, gives the opportunity to further study the targeted molecules in the solid and/or solution state with additional spectroscopic techniques such as NMR (^{1}H, ^{13}C, ^{89}Y) or EPR for the Gd^{III} species. For the present study, ESI-MS studies of compounds **7**, **10** and **16**, are indicative that the targeted species retain intact into the solution. However upon introduction of co-ligands the targeted CCs become insoluble in alcoholic solvents. Computational studies showcasing how the likely activity of the CCs can be tuned and modulated and suggesting ways on achieving this, hence demonstrating the richness of the chemistry of the hereby reported constructs. Our future efforts will be focused on further exploring the coordination chemistry of these species as well to perform such systematic studies involving other organic ligands, aiming to isolate molecules with better magnetic, catalytic or fluorescent properties.

Experimental

Materials. Chemicals (reagent grade) were purchased from Sigma Aldrich and Alfa Aesar. Detailed synthesis and characterization of the HL ligand is described in the ESI. All experiments were performed under aerobic conditions using materials and solvents as received. *Safety note*: Perchlorate salts are potentially explosive; such compounds should be used in small quantities and handled with caution and utmost care at all times.

Synthesis. Detailed synthetic protocols can be found in the Supporting information. Powder XRD spectra of the compounds **4** – **21** were not recorded, due to the fact that these molecules can be considered as unexpected reaction products. Elemental analysis results of selected samples (**7**, **10**, **11**, **13** and **16**) are reported in the ESI.

Instrumentation. IR spectra of the samples were recorded over the range of 4000-650 cm^{-1} on a Perkin Elmer Spectrum One FT-IR spectrometer fitted with a UATR polarization accessory.

Computational Details. Energy minimization on strategically designed model compounds (see Results and Discussion) were conducted within the Kohn-Sham Density Functional Theory (DFT) approach at the B3LYP/SDD and B3LYP/6-311G* levels.[77–87] Calculations were carried using the Gaussian09[88] software. The Jmol program was used for visualization purposes.[89]

X-ray Crystallography. Data for **H_2L3**, **H_2L19**, **5** – **8**, **10** – **12**, **15** – **17** and **21** were collected (ω- scans) at the University of Sussex using an Agilent Xcalibur Eos Gemini Ultra diffractometer with CCD plate detector under a flow of nitrogen gas at 173(2) K using Mo Kα radiation (λ = 0.71073 Å). CRYSALIS CCD and RED software was used respectively for data collection and processing. Reflection intensities were corrected for absorption by the multi-scan method. Data for **4**, **9**, **13**, **14**, **18** – **20** were collected at the National Crystallography Service, University of Southampton.[90] All structures were determined using Olex2[91], solved using either Superflip[92] or SHELXT[93,94] and refined with SHELXL-2014.[95] All non-H atoms were refined with anisotropic thermal parameters, and H-atoms were introduced at calculated positions and allowed to ride on their carrier atoms. Geometric/crystallographic calculations were performed using PLATON[96], Olex2[91], and WINGX[93] packages; graphics were prepared with Crystal Maker.[97] For compounds **8**, **9** and **14** the SQUEEZE process was applied.[98] Each of the crystal structures has been deposited at the CCDC 1406218-1406237.

Acknowledgements

We thank the EPSRC (UK) for funding (grant number EP/M023834/1), the University of Sussex for offering a PhD position to K.G., the EPSRC UK National Crystallography Service at the University of Southampton for the collection of the crystallographic data for compounds **4**, **9**, **13**, **14**, **18** – **20**, the Research Development Funding from the University of Sussex (V. N. D.) and Profs Vladislav Blatov and Davide Proserpio for helpful discussions.

Notes and references

1. L. Cronin and J. Fielden, in *Coordination Clusters in Encyclopedia of Supramolecular Chemistry, Taylor and Francis, London, 2007,* Taylor & Francis, 2007, pp. 1–10.
2. G. E. Kostakis, A. M. Ako, and A. K. Powell, *Chem. Soc. Rev.*, 2010, **39**, 2238–2271.
3. Z.-M. Zhang, S. Yao, Y.-G. Li, R. Clérac, Y. Lu, Z.-M. Su, and E.-B. Wang, *J. Am. Chem. Soc.*, 2009, **131**, 14600–14601.
4. X.-J. Kong, Y.-P. Ren, W.-X. Chen, L.-S. Long, Z. Zheng, R.-B. Huang, and L.-S. Zheng, *Angew. Chem. Int. Ed.*, 2008, **47**, 2398–2401.
5. A. A. Athanasopoulou, M. Pilkington, C. P. Raptopoulou, A. Escuer, and T. C. Stamatatos, *Chem. Commun.*, 2014, **50**, 14942–14945.
6. C.-M. Liu, D.-Q. Zhang, and D.-B. Zhu, *Dalton Trans.*, 2010, **39**, 11325–11328.
7. J.-B. Peng, X.-J. Kong, Q.-C. Zhang, M. Orendáč, J. Prokleška, Y.-P. Ren, L.-S. Long, Z. Zheng, and L.-S. Zheng, *J. Am. Chem. Soc.*, 2014, **136**, 17938–17941.
8. Z. M. Zhang, L. Y. Pan, W. Q. Lin, J. D. Leng, F. S. Guo, Y. C. Chen, J. L. Liu, and M. L. Tong, *Chem. Commun.*, 2013, **49**, 8081–8083.
9. L. Zhao, J. Wu, S. Xue, and J. Tang, *Chem. Asian J.*, 2012, **7**, 2419–2423.
10. M. Wu, F. Jiang, D. Yuan, J. Pang, J. Qian, S. A. Al-Thabaiti, and M. Hong, *Chem. Commun.*, 2014, **50**, 1113–1115.
11. D. D'Alessio, A. N. Sobolev, B. W. Skelton, R. O. Fuller, R. C. Woodward, N. A. Lengkeek, B. H. Fraser, M. Massi, and M. I. Ogden, *J. Am. Chem. Soc.*, 2014, **136**, 15122–15125.
12. E. N. Chygorin, V. N. Kokozay, I. V. Omelchenko, O. V. Shishkin, J. Titiš, R. Boča, and D. S. Nesterov, *Dalt. Trans.*, 2015, **44**, 10918–10922.
13. D. S. Nesterov, E. N. Chygorin, V. N. Kokozay, V. V Bon, R. Boča, Y. N. Kozlov, L. S. Shul'pina, J. Jezierska, A. Ozarowski, A. J. L. Pombeiro, and G. B. Shul'pin, *Inorg. Chem.*, 2012, **51**, 9110–9122.
14. Z. Ma, L. Wei, E. C. B. A. Alegria, L. M. D. R. S. Martins, M. F. C. Guedes da Silva, and A. J. L. Pombeiro, *Dalton Trans.*, 2014, **43**, 4048–4058.
15. G. Maayan and G. Christou, *Inorg. Chem.*, 2011, **50**, 7015–7021.
16. D. S. Nesterov, V. N. Kokozay, J. Jezierska, O. V Pavlyuk, R. Boča, and A. J. L. Pombeiro, *Inorg. Chem.*, 2011, **50**, 4401–4411.
17. J. S. Kanady, E. Y. Tsui, M. W. Day, and T. Agapie, *Science*, 2011, **333**, 733–736.
18. D. I. Alexandropoulos, L. Cunha-Silva, L. Pham, V. Bekiari, G. Christou, and T. C. Stamatatos, *Inorg. Chem.*, 2014, **53**, 3220–3229.
19. X. Yang, Z. Li, S. Wang, S. Huang, D. Schipper, and R. A. Jones, *Chem. Commun.*, 2014, **50**, 15569–15572.
20. J. Jankolovits, C. M. Andolina, J. W. Kampf, K. N. Raymond, and V. L. Pecoraro, *Angew. Chem. Int. Ed.*, 2011, **50**, 9660–9664.
21. G. Guthausen, J. R. Machado, B. Luy, A. Baniodeh, A. K. Powell, S. Krämer, F. Ranzinger, M. P. Herrling, S. Lackner, and H. Horn, *Dalton Trans.*, 2015, **44**, 5032–5040.
22. E. C. Sañudo and L. Rosado Piquer, *Dalton Trans.*, 2015, **44**, 8771–8780.
23. K. Liu, W. Shi, and P. Cheng, *Coord. Chem. Rev.*, 2015, **289-290**, 74–122.
24. A. J. Tasiopoulos and S. P. Perlepes, *Dalton Trans.*, 2008, 5537–5555.
25. L. Zhao, J. Wu, H. Ke, and J. Tang, *Inorg. Chem.*, 2014, **53**, 3519–3525.
26. V. Chandrasekhar, P. Bag, W. Kroener, K. Gieb, and P. Müller, *Inorg. Chem.*, 2013, **52**, 13078–13086.
27. S. Hossain, S. Das, A. Chakraborty, F. Lloret, J. Cano, E. Pardo, and V. Chandrasekhar, *Dalton Trans.*, 2014, **43**, 10164–10174.
28. V. Chandrasekhar, S. Das, A. Dey, S. Hossain, F. Lloret, and E. Pardo, *Eur. J. Inorg. Chem.*, 2013, **2013**, 4506–4514.
29. M. Nematirad, W. J. Gee, S. K. Langley, N. F. Chilton, B. Moubaraki, K. S. Murray, and S. R. Batten, *Dalton Trans.*, 2012, **41**, 13711–13715.
30. M. Towatari, K. Nishi, T. Fujinami, N. Matsumoto, Y. Sunatsuki, M. Kojima, N. Mochida, T. Ishida, N. Re, and J. Mrozinski, *Inorg. Chem.*, 2013, **52**, 6160–6178.
31. M. Sarwar, A. M. Madalan, C. Tiseanu, G. Novitchi, C. Maxim, G. Marinescu, D. Luneau, and M. Andruh, *New J. Chem.*, 2013, **37**, 2280–2292.
32. L.-L. Fan, F.-S. Guo, L. Yun, Z.-J. Lin, R. Herchel, J.-D. Leng, Y.-C. Ou, and M.-L. Tong, *Dalton Trans.*, 2010, **39**, 1771–1780.
33. L. Zhao, S. Xue, and J. Tang, *Inorg. Chem.*, 2012, **51**, 5994–5996.
34. L.-F. Zou, L. Zhao, Y.-N. Guo, G.-M. Yu, Y. Guo, J. Tang, and Y.-H. Li, *Chem. Commun.*, 2011, **47**, 8659–8661.
35. F. Habib, G. Brunet, V. Vieru, I. Korobkov, L. F. Chibotaru, and M. Murugesu, *J. Am. Chem. Soc.*, 2013, **135**, 13242–13245.
36. J.-P. Costes and C. Duhayon, *Eur. J. Inorg. Chem.*, 2014, 4745–4749.
37. V. Gómez, L. Vendier, M. Corbella, and J.-P. Costes, *Inorg. Chem.*, 2012, **51**, 6396–6404.
38. E. Loukopoulos, B. Berkoff, A. Abdul-Sada, G. J. Tizzard, S. J. Coles, A. Escuer, and G. E. Kostakis, *Eur. J. Inorg. Chem.*, 2015, 2646–2649.
39. B. Berkoff, K. Griffiths, A. Abdul-Sada, G. J. Tizzard, S. Coles, A. Escuer, and G. E. Kostakis, *Dalton Trans.*, 2015, **44**, 12788–12795.
40. M. Andruh, *Dalton Trans.*, 2015, **44**, 16633–16653.
41. J. Wu, L. Zhao, P. Zhang, L. Zhang, M. Guo, and J. Tang, *Dalton Trans.*, 2015, **44**, 11935–11942.
42. H. Wang, H. Ke, S.-Y. Lin, Y. Guo, L. Zhao, J. Tang, and Y.-H. Li, *Dalton Trans.*, 2013, **42**, 5298–5303.
43. P. Zhang, L. Zhang, S.-Y. Lin, and J. Tang, *Inorg. Chem.*, 2013, **52**, 6595–6602.
44. H. Ke, L. Zhao, Y. Guo, and J. Tang, *Dalton Trans.*, 2012, **41**, 2314–2319.
45. H. Ke, L. Zhao, Y. Guo, and J. Tang, *Dalton Trans.*, 2012, **41**, 9760–9765.
46. K. C. Mondal, A. Sundt, Y. Lan, G. E. Kostakis, O. Waldmann, L. Ungur, L. F. Chibotaru, C. E. Anson, and A. K. Powell, *Angew. Chem. Int. Ed.*, 2012, **51**, 7550 –7554.
47. K. C. Mondal, G. E. Kostakis, Y. Lan, W. Wernsdorfer, C. E. Anson, and A. K. Powell, *Inorg. Chem.*, 2011, **50**, 11604–11611.
48. K. C. Mondal, G. E. Kostakis, Y. Lan, and A. K. Powell, *Polyhedron*, 2013, **66**, 268–273.
49. H. Ke, L. Zhao, Y. Guo, and J. Tang, *Inorg. Chem.*, 2012, **51**, 2699–2705.
50. H. Ke, W. Zhu, S. Zhang, G. Xie, and S. Chen, *Polyhedron*, 2015, **87**, 109–116.
51. R. Kannappan, D. M. Tooke, A. L. Spek, and J. Reedijk, *Inorg. Chim. Acta*, 2006, **359**, 334–338.
52. I. Nemec, M. Machata, R. Herchel, R. Boča, and Z. Trávníček, *Dalton Trans.*, 2012, **41**, 14603–14610.
53. N. Kushwah, M. K. Pal, A. Wadawale, V. Sudarsan, D. Manna, T. K. Ghanty, and V. K. Jain, *Organometallics*, 2012, **31**, 3836–3843.
54. S. Saha, S. Pal, C. J. Gómez-García, J. M. Clemente-Juan, K.

Harms, and H. P. Nayek, *Polyhedron*, 2014, **74**, 1–5.
55. M. Hasanzadeh, M. Salehi, M. Kubicki, S. M. Shahcheragh, G. Dutkiewicz, M. Pyziak, and A. Khaleghian, *Trans Met. Chem.*, 2014, **39**, 623–632.
56. D. Dey, G. Kaur, A. Ranjani, L. Gayathri, P. Chakraborty, J. Adhikary, J. Pasan, D. Dhanasekaran, A. R. Choudhury, M. A. Akbarsha, N. Kole, and B. Biswas, *Eur. J. Inorg. Chem.*, 2014, 3350–3358.
57. K. Griffiths, C. W. D. Gallop, A. Abdul-Sada, A. Vargas, O. Navarro, and G. E. Kostakis, *Chem. Eur. J.*, 2015, **21**, 6358–6361.
58. P. King, R. Clerac, W. Wernsdorfer, C. E. Anson, and A. K. Powell, *Dalton Trans.*, 2004, 2670–2676.
59. G. E. Kostakis and A. K. Powell, *Coord. Chem. Rev.*, 2009, **253**, 2686–2697.
60. G. E. Kostakis, V. A. Blatov, and D. M. Proserpio, *Dalton Trans.*, 2012, **41**, 4634–4640.
61. O. M. Yaghi, M. O'Keeffe, N. W. Ockwig, H. K. Chae, M. Eddaoudi, and J. Kim, *Nature*, 2003, **423**, 705–714.
62. R. Della Pergola, F. Demartin, L. Garlaschelli, M. Manassero, S. Martinengo, N. Masciocchi, and D. Strumolo, *Inorg. Chem.*, 1991, **30**, 846–849.
63. D. Collini, F. F. De Biani, S. Fedi, C. Femoni, F. Kaswalder, M. C. Iapalucci, G. Longoni, C. Tiozzo, S. Zacchini, and P. Zanello, *Inorg. Chem.*, 2007, **46**, 7971–7981.
64. J. L. Atwood and J. W. Steed, in *Supramolecular Chemistry, 2nd Edition*, 2009, p. 402.
65. S. Bhattacharya and B. K. Saha, *CrystEngComm*, 2011, **13**, 6941–6944.
66. A. J. Close, P. Kemmitt, M. K. Emmerson, and J. Spencer, *Tetrahedron*, 2014, **70**, 9125–9131.
67. K. Branko and Z. Marija, *Acta Chim. Slov.*, 2012, **59**, 670–679.
68. G. T. Tigineh, Y.-S. Wen, and L.-K. Liu, *Tetrahedron*, 2015, **71**, 170–175.
69. J. Spencer, N. Anjum, H. Patel, R. Rathnam, and J. Verma, *Synlett*, 2007, 2557–2558.
70. J. Spencer, C. B. Baltus, H. Patel, N. J. Press, S. K. Callear, L. Male, and S. J. Coles, *ACS Comb. Sci.*, 2011, **13**, 24–31.
71. C. C. Stoumpos, T. C. Stamatatos, H. Sartzi, O. Roubeau, A. J. Tasiopoulos, V. Nastopoulos, S. J. Teat, G. Christou, and S. P. Perlepes, *Dalton Trans.*, 2009, 1004–1015.
72. G. S. Papaefstathiou, C. P. Raptopoulou, A. Tsohos, A. Terzis, E. G. Bakalbassis, and S. P. Perlepes, *Inorg. Chem.*, 2000, **39**, 4658–4662.
73. T. C. Stamatatos, K. A. Abboud, S. P. Perlepes, and G. Christou, *Dalton Trans.*, 2007, 3861–3863.
74. G. C. Vlahopoulou, T. C. Stamatatos, V. Psycharis, S. P. Perlepes, and G. Christou, *Dalton Trans.*, 2009, 3646–3649.
75. W.-H. Zhu, Y. Zhang, Z. Guo, S. Wang, J. Wang, Y.-L. Huang, L. Liu, Y.-Q. Fan, F. Cao, and S.-W. Xiang, *RSC Adv.*, 2014, **4**, 49934–49941.
76. J. Tönnemann, J. Risse, Z. Grote, R. Scopelliti, and K. Severin, *Eur. J. Inorg. Chem.*, 2013, **2013**, 4558–4562.
77. A. D. Becke, *J. Chem. Phys.*, 1993, **98**, 1372–1377.
78. A. D. McLean and G. S. Chandler, *J. Chem. Phys.*, 1980, **72**, 5639–5648.
79. R. Krishnan, J. S. Binkley, R. Seeger, and J. A. Pople, *J. Chem. Phys.*, 1980, **72**, 650–654.
80. A. J. H. Wachters, *J. Chem. Phys.*, 1970, **52**, 1033–1066.
81. P. J. Hay, *J. Chem. Phys.*, 1977, **66**, 4377–4384.
82. K. Raghavachari and G. W. Trucks, *J. Chem. Phys.*, 1989, **91**, 1062–1065.
83. T. Clark, J. Chandrasekhar, G. W. Spitznagel, and P. V. R. Schleyer, *J. Comput. Chem.*, 1983, **4**, 294–301.
84. M. J. Frisch, J. A. Pople, and J. S. Binkley, *J. Chem. Phys.*, 1984, **80**, 3265–3269.
85. P. Fuentealba, H. Preuss, H. Stoll, and L. Von Szentpály, *Chem. Phys. Lett.*, 1982, **89**, 418–422.
86. U. Wedig, M. Dolg, H. Stoll, and H. Preuss, *Quantum Chemistry: The Challenges of Transition Metals and Coordination Chemistry,* Dordrecht.
87. M. F. Summers, *Coord. Chem. Rev.*, 1988, **86**, 43–134.
88. M. Frisch, G. Trucks, and H. Schlegel, *Gaussian Inc., Wallingford …*, 2010.
89. http://jmol.sourceforge.net/
90. S. J. Coles and P. A. Gale, *Chem. Sci.*, 2012, **3**, 683–689.
91. O. V Dolomanov, A. J. Blake, N. R. Champness, and M. Schröder, *J. Appl. Crystallogr.*, 2003, **36**, 1283–1284.
92. L. Palatinus and G. Chapuis, *J. Appl. Crystallogr.*, 2007, **40**, 786–790.
93. L. J. Farrugia, *J. Appl. Crystallogr.*, 1999, **32**, 837–838.
94. G. M. Sheldrick, *Acta Crystallogr. Sect. A Found. Adv.*, 2015, **71**, 3–8.
95. G. M. Sheldrick, *Acta Crystallogr. Sect. A*, 2008, **64**, 112–122.
96. A. L. Spek, *J. Appl. Crystallogr.*, 2003, **36**, 7–13.
97. C. F. Macrae, P. R. Edgington, P. McCabe, E. Pidcock, G. P. Shields, R. Taylor, M. Towler, and J. Van De Streek, *J. Appl. Crystallogr.*, 2006, **39**, 453–457.
98. A. L. Spek, *Acta Crystallogr. D. Biol. Crystallogr.*, 2009, **65**, 148–155.